A numerical study of the wind field in a typhoon boundary layer

Yan Meng*, Masahiro Matsui, Kazuki Hibi

*Environmental Engineering Department, Institute of Technology, Shimizu Corporation,
No. 4-17, Etchujima, 3-chome, Koto-ku. Tokyo 135, Japan*

Abstract

The wind field in a typhoon boundary layer (TBL) has been investigated by a numerical model. The results show that vertical profiles of wind speed in the TBL can be satisfactorily stated by conventional power-law expressions. To describe the structure of strong wind in the TBL, two parameters have been suggested: one is a dimensional parameter, f_λ, approximately representing the absolute vorticity in the wind field, and the other is a non-dimensional parameter, ξ, characterizing the heterogeneity of vorticity in the radial direction of a typhoon. Substituting the parameter f_λ by Coriolis parameter f, the gradient height z_g during typhoons can be predicted by the same formula as that used during non-typhoon climates. The ratio of surface to gradient wind speeds $G(r)$ and the inflow angle γ_s in the TBL are also examined using the present numerical results, and the formulae for predicting them are presented.

Keywords: Typhoon boundary layer; New external parameters; Prediction of the vertical wind profile; Ratio of surface to gradient wind speeds; Inflow angle

Nomenclature

v_θ, v_r	horizontal components of wind
$v_{\theta g}, v_{rg}$	horizontal components of gradient wind
v'_θ, v'_r	differences between wind velocities and gradient winds
v''_θ, v''_r, v''_z	velocity fluctuations
c	translation velocity of typhoon
θ	angle, counterclockwise positive from east
r	radial distance from typhoon center
z	elevation

* Corresponding author. E-mail: meng@sit.shimz.co.jp.

β	approach angle of typhoon, counterclockwise positive from east
γ	inflow angle or geostrophic angle
r_m	radius of maximum wind
f	Coriolis parameter
u_*	friction velocity at the surface
z_0	roughness length
κ	von Karman constant, 0.4
U	wind speed
K_m	turbulent exchange coefficient
q^2	twice the turbulent energy
σ_u	standard deviation of the fluctuation of wind speed
l	master turbulence length scale
l_0	master turbulence length scale as z approaches infinity
B_1	closure parameter, 21.3, see Eq. (7)
S_q	closure parameter, 0.2, see Eq. (8)
α	empirical parameter, 0.1, see Eq. (11)
γ_1	closure parameter, 0.222, see Eq. (12)
f_λ, ξ	see Eqs. (13) and (14)
Ro_λ	modified surface Rossby number
$G(r)$	ratio of surface to gradient wind speeds
U_g	gradient wind speed
z_g	gradient height used in power law expression
α_u	power law exponent for the wind speed profile

1. Introduction

It is well known that in most areas on the southeastern coasts of China and Japan, strong winds are associated with two types of weather systems. The first of these is called the non-typhoon wind climate and represents all winds not related to tropical storms or typhoons. The second type of wind climate is referred to as the typhoon wind climate and represents tropical cyclones originating in the Pacific Ocean. To exactly evaluate wind loads on structures in these regions, a detailed understanding of wind structure in both types of weather systems is required.

During the last few decades, extensive research on wind structure during strong wind conditions has been carried out by meteorologists and engineers. As a result, valuable data for various types of terrain have been gathered from sites, and several empirical models for expression of the vertical profiles of wind speed have been proposed. However, most of them are designed for strong winds in non-typhoon conditions. Information on wind structure during severe tropical cyclones is still insufficient, although Choi [1] has reported some upper-level wind data during typhoons from radar sounding records.

In the present study, a series of numerical simulations are conducted to provide an adequate description of the vertical wind profile during a typhoon. New parameters

are suggested to describe the structure of strong wind in the typhoon boundary layer (TBL). The relation between basic parameters of the power law and external parameters of the TBL are then examined using the numerical results. Finally, the ratio of surface to gradient wind speeds $G(r)$ and the inflow angle γ_s in the TBL are also investigated and formulae for predicting them are presented.

2. Numerical model

2.1. Description of model

A model for describing wind field in the typhoon boundary layer has been proposed by the authors [2]. Fig. 1 is a brief illustration of the model, in which the typhoon-induced mean wind velocity v is expressed by the addition of the gradient wind v_g in the free atmosphere, and the component v', caused by friction on the ground surface. Assuming that the gradient wind pattern moves at the translation velocity of typhoon c in the free atmosphere, gradient wind velocity v_g was analytically obtained by means of perturbation analysis. Furthermore, the equation for the component v' was linearized, considering that the unsteady term in this equation is smaller than the

N. S. equation

$$\frac{\partial \vec{v}}{\partial t} + \vec{v} \cdot \nabla \vec{v} = -\frac{1}{\rho}\nabla p - f\vec{k} \times \vec{v} + \vec{F}$$

$$\vec{v} = \vec{v}_g + \vec{v}'$$

Gradient Wind

$$\frac{\partial \vec{v}_g}{\partial t} + \vec{v}_g \cdot \nabla \vec{v}_g = -\frac{1}{\rho}\nabla p - f\vec{k} \times \vec{v}_g$$

Surface Wind

$$\frac{\partial \vec{v}'}{\partial t} + \vec{v}' \cdot \nabla \vec{v}' + \vec{v}' \cdot \nabla \vec{v}_g + \vec{v}_g \cdot \nabla \vec{v}' = -f\vec{k} \times \vec{v}' + \vec{F}$$

$$\frac{\partial \vec{v}_g}{\partial t} = -\vec{c} \cdot \nabla \vec{v}_g$$

Modeling

$$\frac{\partial \vec{v}'}{\partial t} = 0$$

$$(\vec{v}_g - \vec{c}) \cdot \nabla \vec{v}_g = -\frac{1}{\rho}\nabla p - f\vec{k} \times \vec{v}_g$$

$$\vec{v}' \cdot \nabla \vec{v}' + \vec{v}' \cdot \nabla \vec{v}_g + \vec{v}_g \cdot \nabla \vec{v}' = -f\vec{k} \times \vec{v}' + \vec{F}$$

Perturbation
Analysis

$$-\frac{v_{\theta g}^2}{r} + \frac{v_{\theta g}c_\theta}{r} = -\frac{1}{\rho}\frac{\partial p}{\partial r} + fv_{\theta g}$$

$$v_{rg} = 0$$

$$-(2\frac{v_{\theta g}}{r} + f)v'_\theta = \frac{\partial}{\partial z}(K_m\frac{\partial v'_r}{\partial z})$$

$$(\frac{\partial v_{\theta g}}{\partial r} + \frac{v_{\theta g}}{r} + f)v'_r = \frac{\partial}{\partial z}(K_m\frac{\partial v'_\theta}{\partial z})$$
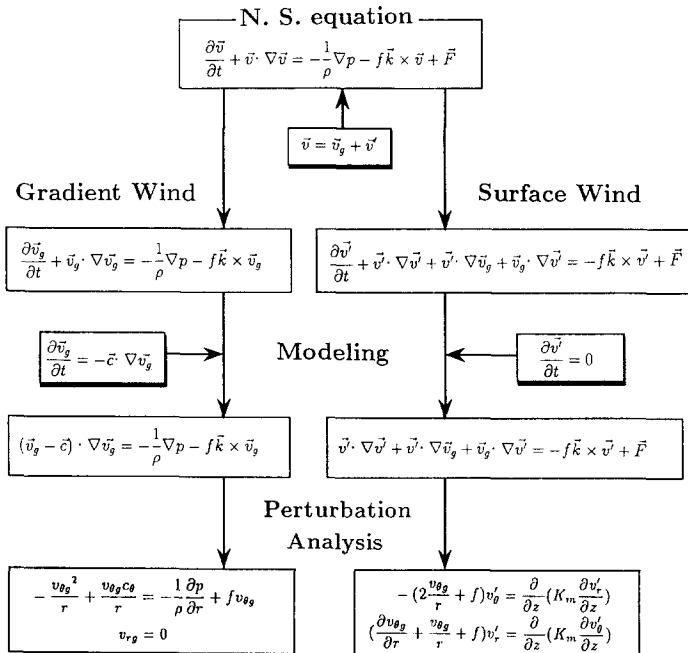
Fig. 1. Summary of the model describing wind field during a typhoon.

turbulent viscosity term and the inertia term, and the component v' is smaller than the gradient wind velocity v_g. Detailed explanations of the typhoon model are described in Ref. [2].

Consequently, gradient wind velocity v_g is expressed as

$$v_{\theta g} = \frac{c_\theta - fr}{2} + \sqrt{\left(\frac{c_\theta - fr}{2}\right)^2 + \frac{r}{\rho}\frac{\partial p}{\partial r}}, \tag{1}$$

$$v_{rg} = 0, \tag{2}$$

and the equation of motion for v' is written as

$$-\left(2\frac{v_{\theta g}}{r} + f\right)v'_\theta = \frac{\partial}{\partial z}\left(K_m\frac{\partial v'_r}{\partial z}\right), \tag{3}$$

$$\left(\frac{\partial v_{\theta g}}{\partial r} + \frac{v_{\theta g}}{r} + f\right)v'_r = \frac{\partial}{\partial z}\left(K_m\frac{\partial v'_\theta}{\partial z}\right), \tag{4}$$

where $c_\theta = -c\sin(\theta - \beta)$. Fig. 2 shows the coordinate system used in this study. Approach angle β and angle θ are defined as counterclockwise positive from the east. The boundary condition at the upper atmosphere is

$$v'|_{z\to\infty} = 0 \tag{5}$$

and the boundary condition above the ground surface is obtained from the logarithmic formula

$$U = \frac{u_*}{\kappa}\ln\frac{z}{z_0}, \tag{6}$$
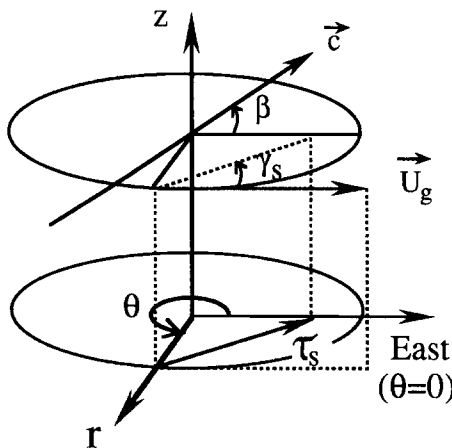
Fig. 2. Coordinate system.

in which $U\ (= \sqrt{v_\theta^2 + v_r^2})$ is zero wind speed at $z = z_0$, κ is the von Karman constant, and u_* is the von Karman friction velocity at the surface.

The expression of the vertical distribution of K_m is an important factor for successful simulations of the atmospheric boundary layer (ABL). The present study used a turbulence closure model proposed by Mellor and Yamada [3] in which K_m is related to turbulence kinetic energy $q^2/2$ and turbulence length l through the expression

$$K_m = B_1^{-1/3} q l, \tag{7}$$

and $q^2/2$ is obtained by solving the turbulence kinetic energy equation as follows:

$$\frac{\partial}{\partial z}\left(q l S_q \frac{\partial q^2/2}{\partial z}\right) - \overline{v_\theta'' v_z''} \frac{\partial v_\theta}{\partial z} - \overline{v_r'' v_z''} \frac{\partial v_r}{\partial z} - \frac{q^3}{B_1 l} = 0, \tag{8}$$

in which $-\overline{v_\theta'' v_z''}$ and $-\overline{v_r'' v_z''}$ are turbulence second moments obtained from a set of diagnostic equations and are expressed as

$$(-\overline{v_\theta'' v_z''},\ -\overline{v_r'' v_z''}) = B_1^{-1/3} q l \left(\frac{\partial v_\theta}{\partial z}, \frac{\partial v_r}{\partial z}\right). \tag{9}$$

For turbulence length scale l, Blackadar's interpolation formula is adapted as

$$l = \frac{\kappa z}{1 + \kappa z/l_0}, \tag{10}$$

which interpolates between two limits $l \to \kappa z$ as $z \to 0$ and $l \to l_0$ as $z \to \infty$. l_0 is assumed to be proportional to the ratio of the first to the zeroth moment of the profile $q(z)$. Thus,

$$l_0 = \alpha \frac{\displaystyle\int_0^\infty z q\,\mathrm{d}z}{\displaystyle\int_0^\infty q\,\mathrm{d}z}, \tag{11}$$

where α is an empirical constant and is set as 0.1. This expression works well for the boundary layer, as pointed out by Mellor and Yamada [3].

The standard deviation of the fluctuation of wind speed is obtained as

$$\sigma_u^2 = (1 - 2\gamma_1) q^2. \tag{12}$$

The values of closure parameters $(B_1, S_q, \gamma_1) = (21.3, 0.2, 0.222)$ have been determined from neutral turbulence data.

Finite-difference methods are used to obtain the numerical solution. The space derivative terms are approximated with central differences, and all equations are iteratively solved by the successive over relaxation (SOR) method.

2.2. External parameters in the TBL

In order to describe the structures of strong wind in the TBL, the following two parameters are introduced,

$$f_\lambda = \left(\frac{\partial v_{\theta g}}{\partial r} + \frac{v_{\theta g}}{r} + f\right)^{1/2} \left(2\frac{v_{\theta g}}{r} + f\right)^{1/2}, \tag{13}$$

$$\xi = \left(2\frac{v_{\theta g}}{r} + f\right)^{1/2} \bigg/ \left(\frac{\partial v_{\theta g}}{\partial r} + \frac{v_{\theta g}}{r} + f\right)^{1/2}, \tag{14}$$

and rearranging Eqs. (3) and (4) gives

$$-\xi f_\lambda v'_\theta = \frac{\partial}{\partial z}\left(K_m \frac{\partial v'_r}{\partial z}\right), \tag{15}$$

$$\frac{1}{\xi} f_\lambda v'_r = \frac{\partial}{\partial z}\left(K_m \frac{\partial v'_\theta}{\partial z}\right), \tag{16}$$

where f_λ has the same dimension as vorticity and ξ is a non-dimensional parameter.

To investigate the radial dependence of f_λ and ξ, the pressure data of typhoon Mireille, observed at 1600 JST on 27 September 1991 [2], are used to calculate the gradient wind speed. Table 1 summarizes the parameters of the typhoon as obtained from the Japanese Meteorological Agency.

Fig. 3a illustrates a variation of f_λ with r/r_m in the $\theta = \beta$ direction. The dashed line represents a mean value of the Coriolis parameter f in the area dominated by typhoon Mireille. As expected, f_λ shows a large value for small r/r_m and gradually approaches the Coriolis parameter f for large r/r_m. Note from Eq. (13) that f_λ approximately expresses absolute vorticity in the ABL during a typhoon. Since relative vorticity $(\partial v_{\theta g}/\partial r + v_{\theta g}/r)$ associated with the typhoon gradually decreases as the distance away from the typhoon center increases, f_λ reaches a value close to the Coriolis parameter f for large r/r_m. This fact implies that, under typhoon condition, f_λ must be adopted as an external parameter to substitute the Coriolis parameter f. Rapid increase of the vorticity associated with a typhoon at places located near the typhoon center has been reported by Mitsuta et al. [4], and the basic shape of the vorticity is similar to f_λ.

Fig. 3b presents the variation of ξ with r/r_m in the $\theta = \beta$ direction. Although the parameter ξ shows a value close to 1 for both small and large r/r_m, it gives a broad peak in the region $2 < r/r_m < 3$. It is obvious from Eq. (14) that the condition for

Table 1
Summary of typhoon parameters used in this study

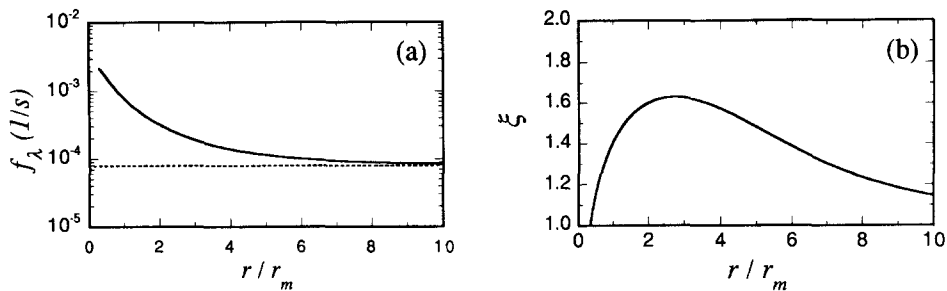| Date (JST)	Time (JST)	Latitude (deg)	Longitude (deg)	β (deg)	C (m/s)	P_c (hPa)	ΔP (hPa)	r_m (km)
91.09.27	16	32.8	129.7	50.1	17.1	940.0	73.0	85.4

Fig. 3. Variation of f_λ and ξ with r/r_m.

$\xi = 1$ is that the distribution of vorticity is uniform in the radial direction. This fact indicates that ξ is a parameter characterizing heterogeneity of vorticity in the radial direction. Since the vorticity field is similar to that induced by solid body motion for small r/r_m and is close to uniform for large r/r_m, this condition is approximately satisfied in both regions. In the region where ξ is larger than 1, the coefficient multiplying v'_θ in Eq. (15) is larger than that multiplying v'_r in Eq. (16). As a result, the inflow angles on the surface do not only depend on the roughness length z_0, but also on the distance away from the typhoon center, as discussed in Section 3.3.

It is well known that, under non-typhoon condition, characteristics of the vertical wind profile in the ABL with neutral stability and horizontal homogeneity depend only on the external parameters, U_g, f, z_0, while, under typhoon condition, the external parameters of the ABL are U_g, f_λ, z_0, ξ. In the next section, our task is to show the wind structure in the TBL and to formulate the relationship between the basic parameters of the power law and these external parameters.

2.3. Code validation

Before moving to the main task, it was necessary to simulate the strong wind records resulting from a developed extratropical depression that occurred at Hokkaido on 4 September 1981, in order to confirm the validity and accuracy of the numerical model. The wind data were obtained from a 213 m high meteorological observation tower located at the center of the Tsukuba Science City. This area is a part of the Kanto Plain, where there is no distinct elevated terrain within a radius of about 20 km. The area within a radius of 150 of the tower is covered with short grass and, farther out, irregular patches of ground are dotted with young pine plantations, no more than 10 m in height.

The wind velocities at six levels (10, 25, 50, 100, 150 and 200 m) were measured by three-dimensional sonic anemometers mounted at the end of 6 m booms extending from the edge of the tower. All signals from the anemometers were sampled at 20 Hz and analyzed by statistical techniques for a run of 100 min in duration. Since the developed extratropical depression was far from the observation site, there were very
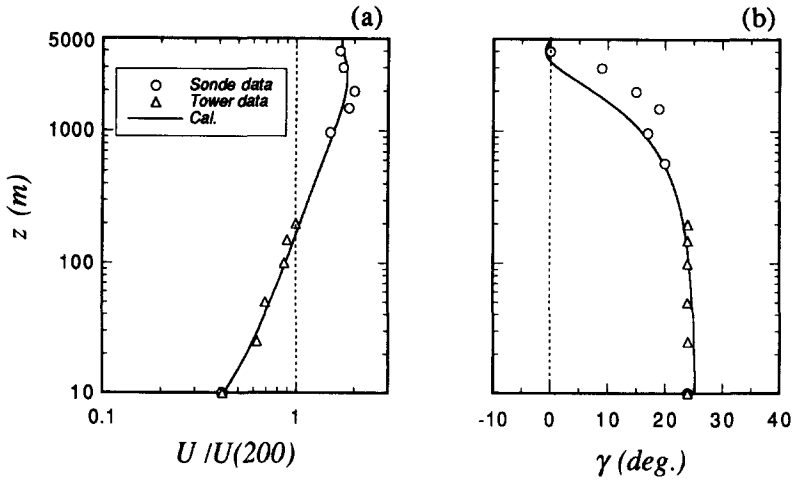
Fig. 4. Comparison of wind speed and direction computed using the numerical model and observed data; symbols: observed; solid line: simulated.

few variations in mean wind speed and direction from 08 : 00 to 17 : 00 h. External parameters of the ABL used in this simulation are set at the following values: $U_g = 27.5$ m/s, $f = 0.857 \times 10^{-4}$ s^{-1}, $z_0 = 0.9$ m. The magnitude of the roughness length z_0 was derived using the log-law to fit the wind speeds obtained at the lower three levels (10, 25 and 50 m).

Fig. 4 shows a comparison of wind speed and wind direction using the numerical results and observed data. Wind speed profiles are normalized by the wind speed at a height of 200 m (top of tower). Agreement between the computed values (solid lines) and observed data (symbols) obtained from the tower is almost total. The validity and accuracy of the numerical model is therefore confirmed.

3. Results and discussion

3.1. An application for simulating typhoon Mireille

The wind field resulting from typhoon Mireille is simulated to examine the radial dependence of the vertical wind profile. The parameters of the typhoon, as shown in Table 1, are used to calculate the gradient wind speed. The roughness length z_0 is set at 0.001, 0.01 and 0.1 m, covering flat coastal areas to rural terrain. Simulations are performed at several typical positions in the radial direction.

Fig. 5a shows the variation of the gradient wind speed and pressure difference with the radius r/r_m. Vertical profiles of wind speed and direction for the case of $z_0 = 0.01$ m are plotted in Fig. 5b and Fig. 5c. Simulated wind speeds (solid lines) are normalized by the gradient wind speed U_g. The dashed lines shown in Fig. 5b and
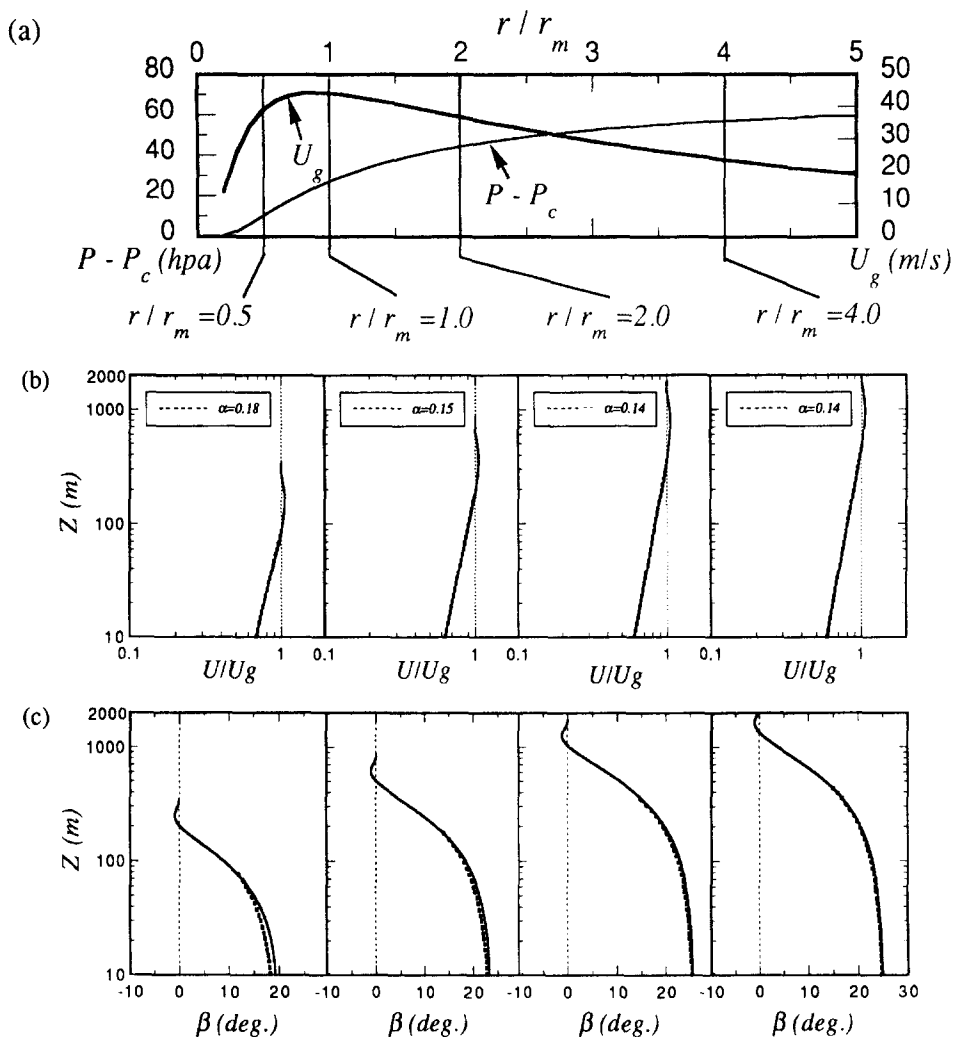
(a)

(b)

(c)

Fig. 5. Vertical profiles of wind speed and direction at several radial locations.

Fig. 5c represent curves calculated using Eqs. (17) and (18),

$$\frac{U(z)}{U_{\mathrm{g}}} = \left(\frac{z}{z_{\mathrm{g}}}\right)^{\alpha_u}, \tag{17}$$

$$\gamma(z) = \gamma_{\mathrm{s}}\left(1.0 - 0.4\frac{z}{z_{\mathrm{g}}}\right)^{1.1}, \tag{18}$$

in which z_{g} denotes the gradient height where the wind speed attains the gradient value. Eq. (17) presents a conventional power-law expression proposed by Davenport [5], and Eq. (18) was suggested by the authors [6,7]. Under the gradient height, the

calculated curves correspond well to the simulated ones. The results indicate that vertical profiles of wind speed and direction in the TBL can also be satisfactorily expressed by the power-law form and Eq. (18).

3.2. Basic parameters of the power law

In this section, the basic parameters of the power law are considered. Fig. 6a shows a variation of the gradient height z_g with radial distance r/r_m for three roughness terrain conditions. It is evident from Fig. 6a that the gradient height z_g has a maximum value at $r/r_m = 4$ and gradually decreases for both small and large r/r_m. The dash-dotted line in Fig. 6a represents the gradient height z_g for the case of $z_0 = 0.01$ m, calculated by the equation $z_g = 0.052 U_g/f (\log Ro)^{-1.45}$. Although this equation has been confirmed to be valid for formulating the gradient height z_g of strong winds under non-typhoon conditions, the predicted gradient height appears to overestimate those obtained from this simulation, especially in the region near the typhoon center. As expected, the basic shape of the predicted gradient is similar to the gradient wind speed shown in Fig. 5a, revealing a gradual increase up to the maximum value at the location near $r = r_m$, and a rapid decrease thereafter. Since overestimation of gradient height results in underestimation of the wind speed in the lower ABL, it is clear that prediction of gradient height is important to evaluating wind loads on engineering structures.

As the authors have previously pointed out [6], gradient height can be expressed as a function of the large length scale of the ABL and surface Rossby number. With the same consideration, the gradient height in the typhoon condition is expressed as

$$z_g = 0.052 \frac{U_g}{f_\lambda} (\log Ro_\lambda)^{-1.45}. \tag{19}$$

Using Eq. (19), the gradient heights are calculated again and shown by solid lines in Fig. 6a. Satisfactory agreement between the calculated values and the numerical results indicates that Eq. (19) is valid.
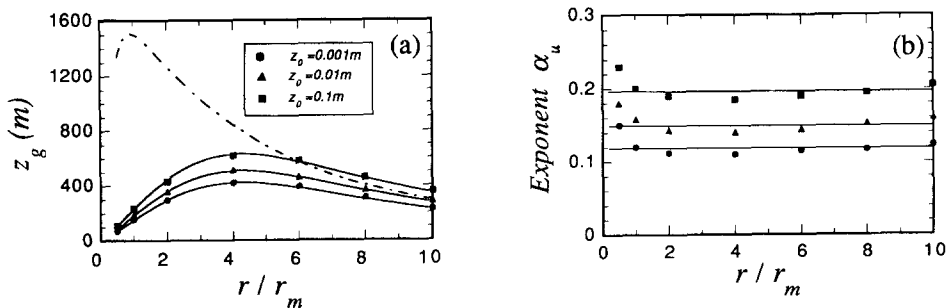

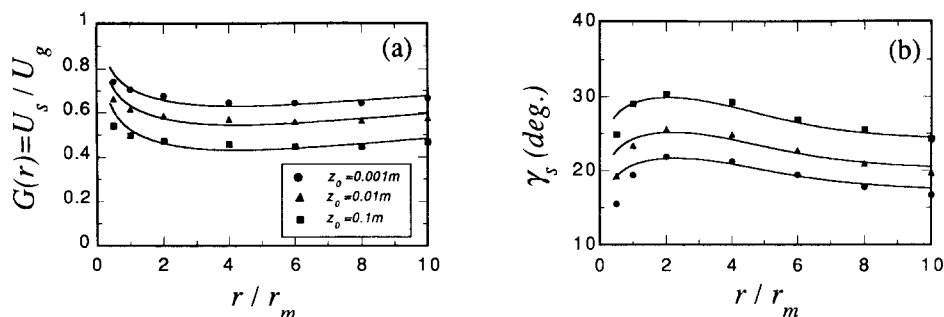Fig. 6. Radial dependence of the gradient height z_g and the power exponent α_u.

Fig. 7. Radial dependence of the wind speed ratio $G(r)$ and the inflow angle γ_s.

The effect of terrain on the shape of the vertical wind profile is represented by the exponent α_u in the power law. Fig. 6b illustrates a variation of the power exponent α_u with r/r_m for three roughness terrain conditions. With the exception of the core region of the typhoon, the power exponents for the three cases are practically steady and can be satisfactorily predicted by Eq. (20) [6],

$$\alpha_u = 0.27 + 0.09 \log z_0 + 0.018(\log z_0)^2 + 0.0016(\log z_0)^3. \tag{20}$$

Although the value of gradient height strongly depends on the large length scale of the ABL, the power exponent can approximately be expressed as a function of the small length scale of the ABL, z_0. If the roughness length z_0 does not change during a typhoon, the power exponents can be expected to be constant and can be predicted from roughness terrain conditions using Eq. (20). This means that if the pressure data associated with a typhoon or hurricane are given, a vertical profile of wind speed and direction at an object site can be readily obtained using the equations given above.

3.3. Wind speed ratio $G(r)$ and inflow angle γ_s

It is well known that wind speed ratio $G(r)$ rapidly increases in the region near the typhoon or hurricane center, as reported by Georgiou et al. [8]. To explain this phenomenon, wind speed ratio $G(r)$ at a height of $z = 10$ m is calculated using the present numerical results, and shown in Fig. 7a. It can be seen that the wind speed ratio $G(r)$ (symbols) obtained from the simulation displays the same tendency as the observation data [8]. Solid lines shown in Fig. 7a are calculated by the power law with fixed exponents obtained by Eq. (20) and gradient heights by Eq. (19), and satisfactorily correspond to the simulated ones. This indicates that rapid increases in wind speed ratio can be explained by abrupt decreases in gradient height in the region near the typhoon or hurricane center.

Fig. 7b presents a variation of the inflow angle γ_s at a height of $z = 10$ m with r/r_m. A broad peak appears at the location $r/r_m = 2$. The shape of the inflow angle γ_s is similar to that of the non-dimensional parameter ξ. Solid lines are calculated by

Eq. (21) and correspond well to simulated ones,

$$\gamma_s = (69 + 100\xi)(\log \mathrm{Ro}_\lambda)^{-1.13}. \tag{21}$$

It is obvious that, in the TBL, the inflow angle γ_s depends not only on the surface Rossby number but also on the non-dimensional parameter ξ.

4. Conclusions

The wind field in a typhoon boundary layer has been investigated by a numerical model. The following summarizes the major findings and conclusions of this study:

1. Two important parameters, f_λ and ξ, have been suggested to describe the structure of strong wind in the TBL. The parameter f_λ approximately represents the absolute vorticity in the ABL, and influences the gradient height. The parameter ξ characterizes the heterogeneity of vorticity in the radial direction and causes an increase in the inflow angle.
2. Vertical profiles of wind speed in the TBL can be satisfactorily stated by the conventional power-law expression. The gradient height is a function of the length scale U_g/f_λ and modified surface Rossby number Ro_λ, and the power exponent can be approximately expressed as a function of the small length scale of the ABL, z_0.
3. The ratio of surface to gradient wind speeds $G(r)$ and the inflow angle γ_s in the TBL are also examined using the present numerical results, and are satisfactorily predicted by the formulas proposed in this study.

References

[1] E.C.C. Choi, Gradient height and velocity profile during typhoons, J. Wind Eng. Ind. Aerodyn. 13 (1983) 31–41.
[2] Y. Meng, M. Matsui, K. Hibi, An analytical model for simulation of the wind field in a typhoon boundary layer, J. Wind Eng. Ind. Aerodyn. 56 (1995) 291–310.
[3] G.L. Mellor, T. Yamada, A hierarchy of turbulence closure models for planetary boundary layer, J. Atmos. Sci. 31 (1974) 1791–1804.
[4] Y. Mitsuta, N. Monji, O. Tsukamoto, H. Asai, Meteorological study of typhoon 7705, Disaster Prevention Research Institute Annuals of Kyoto University, No. 21B, 1978, pp. 405–415 (in Japanese).
[5] A.G. Davenport, The relationship of wind structure to wind loading, Proc. Symp. on Wind Effects on Buildings and Structures, vol. 1, Nalt. Phys. Lab., H.M.S.O., 1965, pp. 53–102.
[6] Y. Meng, M. Matsui, K. Hibi, Characteristics of the vertical wind profile in the neutrally atmospheric boundary layers, Part 1 Strong wind during non-typhoon climates, J. Wind Eng. 65 (1995) 1–15 (in Japanese).
[7] Y. Meng, M. Matsui, K. Hibi, Characteristics of the vertical wind profile in the neutrally atmospheric boundary layers, Part 2 Strong winds during typhoon climates, J. Wind Eng. 66 (1996) 3–14 (in Japanese).
[8] P.N. Georgiou, A.G. Davenport, B.J. Vickery, Design wind speeds in regions dominated by tropical cyclones, J. Wind Eng. Ind. Aerodyn. 13 (1983) 139–152.